

Short Communication

Numerical and Experimental Study of Centrifugal Fan Flow Structures and Their Relationship with Machine Efficiency

Tomasz Siwek, Jan Górski, Stanisław Fortuna

AGH University of Science and Technology, Al. Mickiewicza 30, 30-059 Kraków, Poland

Received: 20 June 2013

Accepted: 9 October 2014

Abstract

This paper presents a CFD study on flow characteristics in the centrifugal fan in nominal and off-design conditions. Numerical calculations were carried out using ANSYS CFX package [10]. The numerical model was verified on the grounds of experimental tests using the standard methods to determine the performance curve of centrifugal fans. The following paper also presents the pressure distributions in select cross-sections of a machine, relative velocity, and static pressure profiles inside the rotor blade channels for the full range of flow characteristics.

Keywords: centrifugal fans, CFD simulation, fan performance prediction

Introduction

Centrifugal fans belong to the power working machines group. They convert mechanical work supplied to the impeller into the static pressure increase of the fluid. The principle of fan operation is based on the conservation of momentum equation, worded in what is generally known as the Euler turbo machinery equation [1]. This equation directly interrelates the basic performance of the machine with the flow kinematics through the machine impeller and provides the basis for determining the design point of operation.

In practice, the fan operates under varying conditions of gas supply, covering almost the full range of the performance curve. By introducing the correction terms such as the slip factor [2] and estimation of the losses calculated according to the available semi-empirical models (which were reviewed in detail in monograph [3]), the approximate shape of an actual characteristics of the fan can be determined. It has been shown that these models represent well the level of losses in the near-design conditions, and the

data quality decreases together with an increase departure from the design state. This is a consequence of technological conditions and often erroneous selection of the machine. The intention of the study is to identify and present the structures of the gas flow field in the fan impeller and casing in the variable flow rates from the maximum to the complete throttled flow.

Reliable identification of flow dynamics in the stage provides information allowing us to specify the available models of losses and enables analytical modeling a full range of operating conditions of the fan. It is also important to identify dissipation structures emerging in the flow and reduce them by better geometric configuration of the channels. This increases the machine efficiency and its functionality. It should be noted that the problem of fan energy consumption was found to be significant for many international regulations. Both the European Union in the Commission Regulation No. 327/2011, as well as the United States in the standardizing document ANSI/AMCA Standard 205-12, charged all manufacturers with a duty to produce equipment meeting very high requirements of energy efficiency and performance [4, 5].

*e-mail: siwek@agh.edu.pl

Table 1. Essential dimensions of the fan

Inlet blade width	$b_1=75$ mm
Outlet blade width	$b_2=54$ mm
Inlet blade angle	$\beta_1=8^\circ$
Outlet blade angle	$\beta_2=45^\circ$
Width of fan housing	$B=180$ mm
Inlet duct diameter	$d_s=220$ mm
Inlet rim diameter	$d_r=203$ mm

Our paper presents the preparation of numerical models and experimental validation of centrifugal fan performance characteristics. As a result of the calculations, the full flow characteristics of the machine have been elaborated upon, both in stable and unstable operating conditions of the fan. Moreover, the flow characteristics have been correlated with the particular operating conditions on the fan characteristics.

Numerical Model

Simulations were carried out on a centrifugal fan with backward curving blades and high specific speed equal to 0.47, and an isentropic efficiency of 80%. The essential dimensions of the machine are presented in Fig. 1 and Table 1.

The spatial geometry (3D) of the modeled fan has been prepared in Autodesk Inventor Professional 2012. Three basic solids covering the area of the fluid in the machine were distinguished, i.e. the single blade channel, the volute casing, and the inlet funnel with a segment in the pipeline, as shown in Fig. 2.

CAD geometry was imported into the ANSYS Design Modeler environment and then transferred to the ANSYS

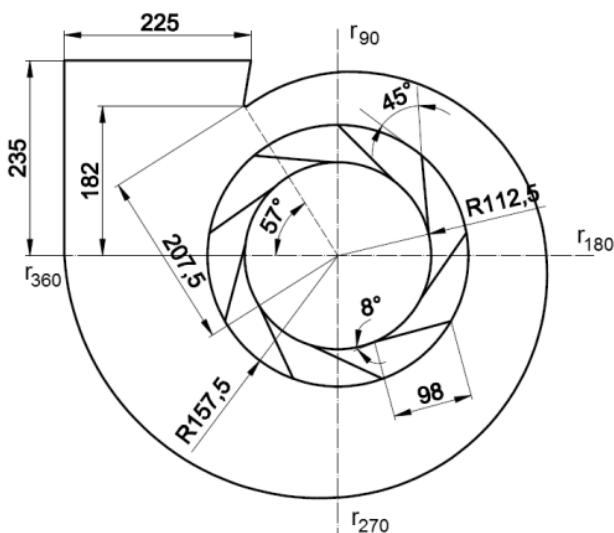


Fig. 1. Cross-section of the test fan.

Mesching [10], where the discretization has been carried out. In the near-wall regions (i.e. front disc, casing walls, and rotor blades), a fine grid was imposed by generating the inflation layer [10], having the first element thickness of 0.5 mm and proliferation ratio of 1.2 for the next 10 sublayers. The total number of the computational grid elements was 3.25×10^6 . Further thickening of the grid was not necessary because of the satisfactory concurrence of the numerical and experimental data. The adopted computing grid is shown in Fig. 3.

The flow through the fan was solved by employing the commercial code ANSYS CFX that uses the finite volume method (FVM). The solution consists of time-averaged Navier-Stokes (RANS) equations. Descriptions of the method and numerical schemes are presented in many handbooks and in [6].

In order to account for the turbulence phenomena in the flow, the k-omega/SST model was selected, which has been recommended in many publications [7-9] and conveys well the flow conditions in the CFD turbo machinery simulation. The SST model (shear stress transport), proposed by Menter [10], takes into account transport of turbulent shear stresses, and helps to get the satisfactory results of numerical simulation of the flow with boundary layer separation (BL) due to rotation and adverse pressure gradient.

An ideal gas model has been used to describe the air properties. Three flow domains have been defined, namely: two stationary domains – inlet pipe and volute casing – and the rotating domain. The boundary conditions have been

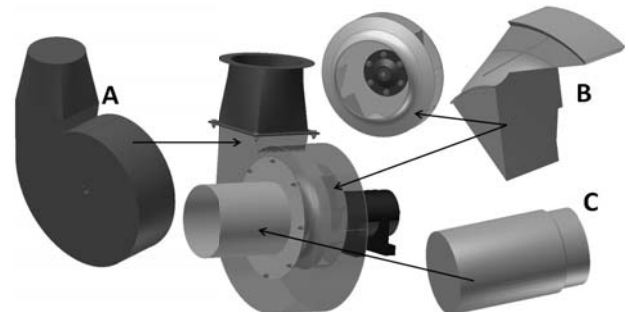


Fig. 2. The simplification of the fan for CFD simulation (A – volute casing, B – blade channel, C – pipeline inlet).

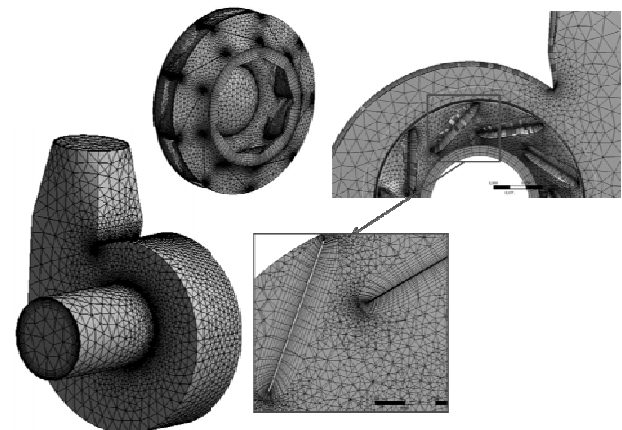


Fig. 3. Numerical grid for the modeled fan geometry.

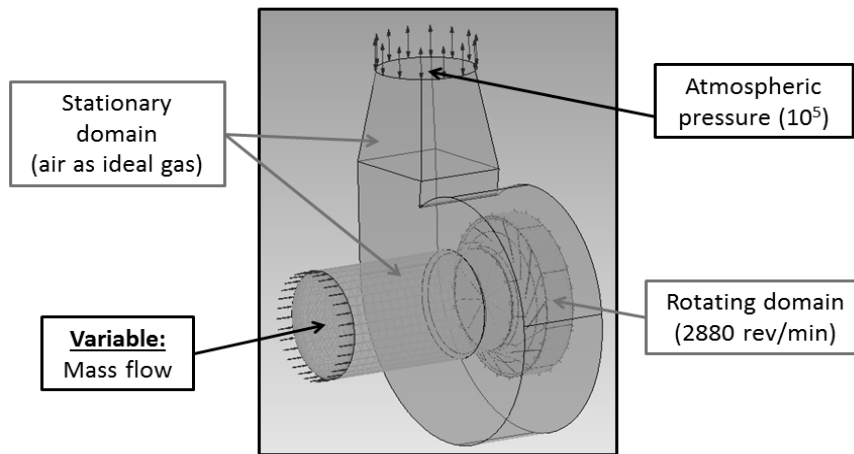


Fig. 4. Defined domains and boundary conditions.

defined as shown in Fig. 4, accepting that at the volute exit the barometric pressure is 100 kPa, the impeller rotational speed of 2880 rev/min, and zero fluid velocity components on the walls. The mass flow was introduced at the inlet as a variable parameter in order to determine the theoretical fan performance curve. An automated-design control of the experiment has been carried out using ANSYS Design Exploration and “what-if” procedure [10]. The mass flow was an input variable and output variables were: the static pressure rise and fan internal efficiency. All calculations have been carried out on the PC (3 processors, 4.2 GHz, 8 GB RAM). Computation time of single point in the fan performance curve was approximately 7 hours.

Numerical Results

As a result of numerical calculations the fan performance curve has been generated and correlated with the previously obtained experimental results. The laboratory experiment was carried out on a test stand according to

DIN EN ISO 5801:2008. In Fig. 5a the relationship between static pressure rise in the stage and the inlet volume flow is presented, and Fig. 5b. shows the internal efficiency of the centrifugal fan (relating to the static parameters).

In analyzing obtained results a proper coincidence of numerical solution with the results of the experiment may be observed. In the near-design conditions, i.e. for the flow close to 0.6 m³/s, the results differ within 1%. The result compliance in the stagnation pressure rise is better in comparison to the efficiency curve. This can be explained by the model simplifications to more favourable form in terms of internal flow aerodynamics (elimination of protruding parts, smoothing welds, no leaks), which limit energy losses. It should be noted that on the pressure rise characteristics some instabilities have been captured, resulting from reaching the surge limit. In Fig. 5a the effect of the number of grid elements on the calculation accuracy was also identified. The first approximation (circles) corresponds to the automatical grid generation case, without the local inflation layers and grid refinement (0.3 million elements).

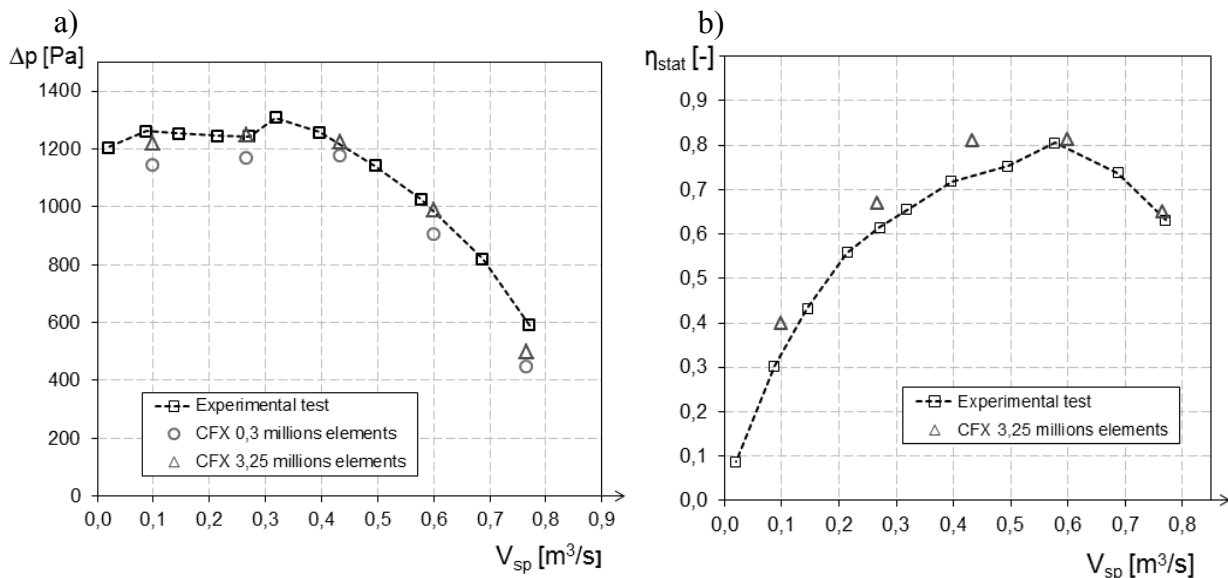


Fig. 5. Fan performance curve – ANSYS CFX and experimental data: a) pressure vs. flow, b) internal efficiency (symbols: square – experimenter, circle/triangle – CFD/CFX).

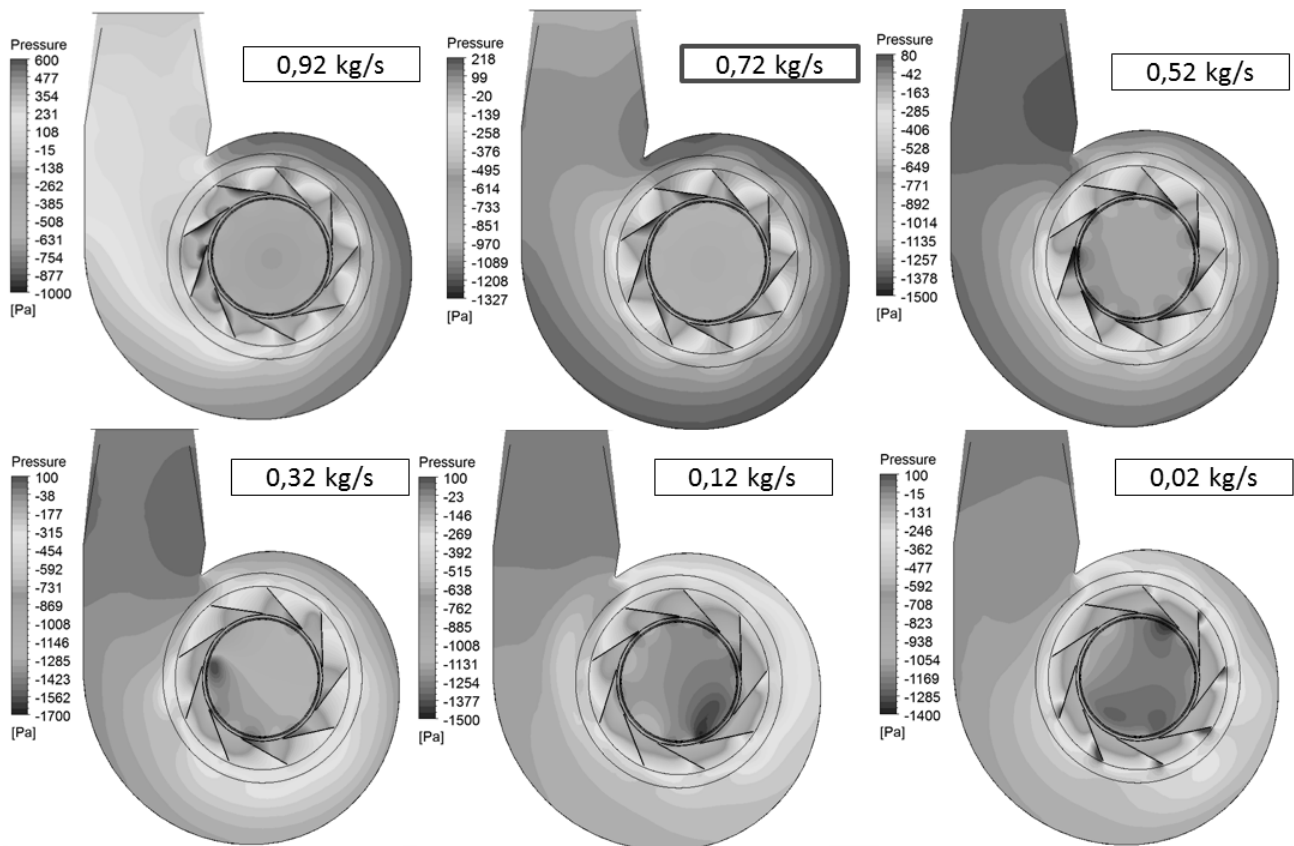


Fig. 6. Pressure contours in the fan cross-section ($b_2/2$) for different operating points.

The accuracy of calculations for this model in the design point was of $\sim 9\%$ of error. For the fine grid and over 3 million elements, the numerically generated pressure rise curve is correct both qualitatively as well as quantitatively.

The confrontation of numerical and experimental results has confirmed the rightness of the applied numerical model. The next step of the investigation presents the flow

structures in the impeller blade channels and the fan housing that have been generated based on the results of the subsequent numerical simulation.

Fig. 6 presents the pressure distribution in the cross-section of the fan (50% of blade width at the impeller outlet – b_2), for the selected six operating points covering the whole range of fan performance characteristics.

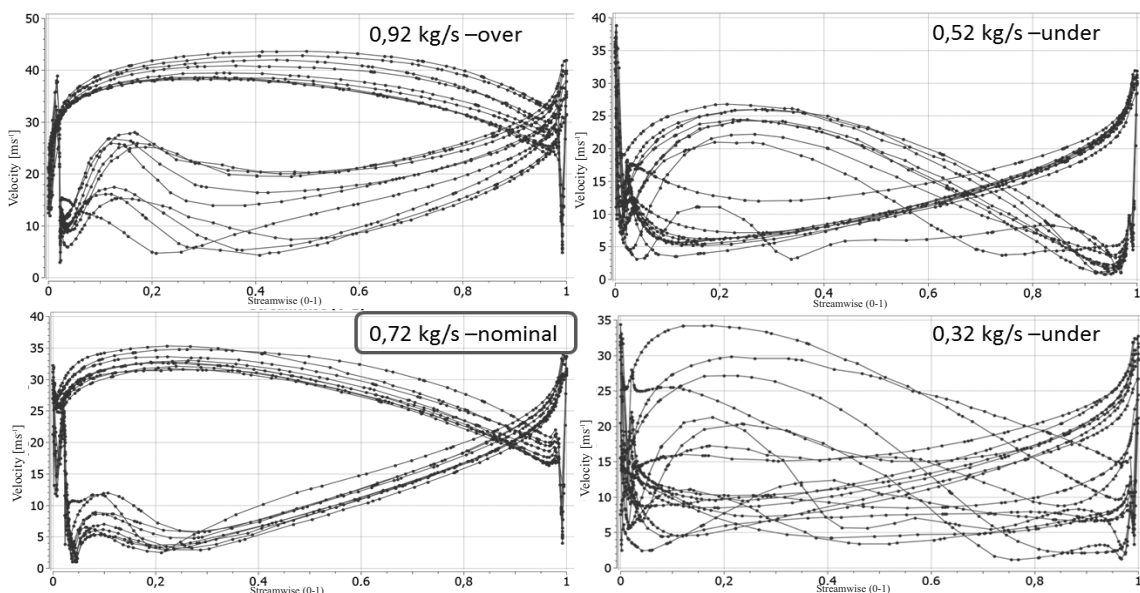


Fig. 7. Relative velocity distribution in the rotor blade channels (50% of b_2).

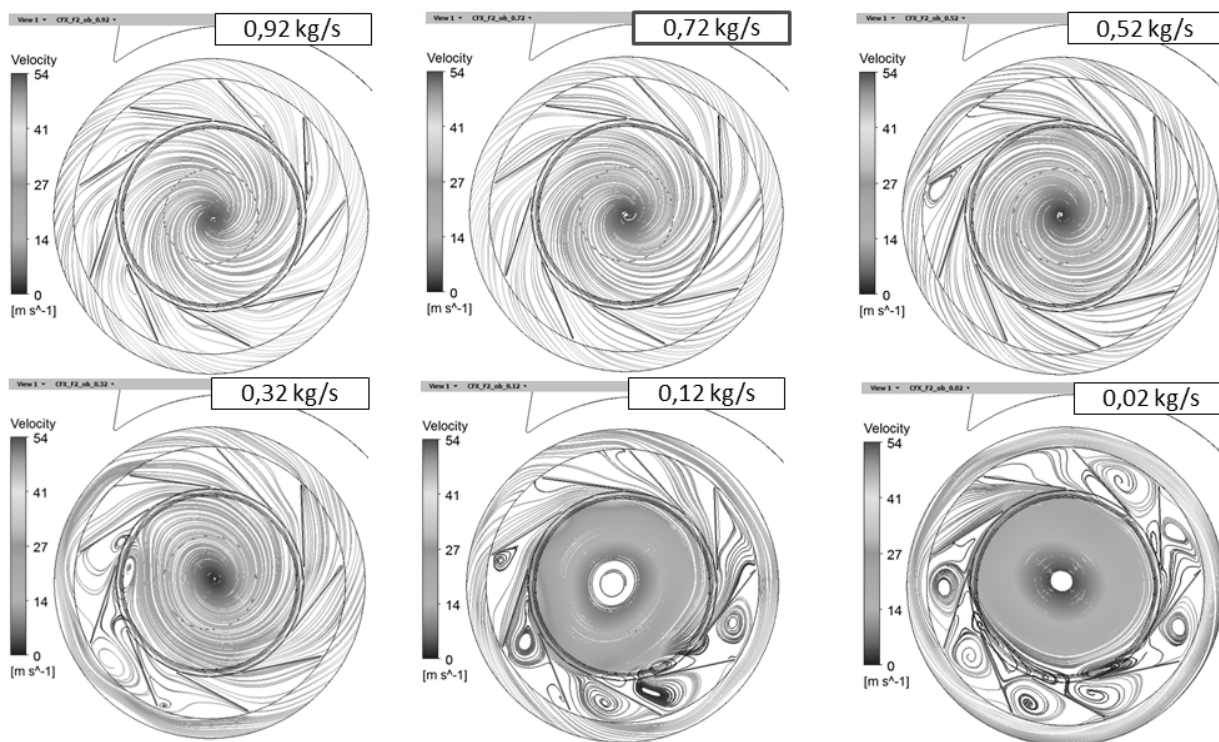


Fig. 8. Vortex structures in the inter-blade passages.

In analyzing the pressure distribution it can be concluded that for the nominal point (0.72 kg/s) it is symmetrical for the entire cross-section in each blade channel of the impeller. In the case of over-nominal flow some local pressure gradients at the impeller exit and volute part are formed. This causes an asymmetry in the outlet pressure distribution from the impeller, the occurrence of the low pressure regions in this area of the rotor, and the exit section of volute casing. In the case of sub nominal flow conditions, an asymmetry of pressure distribution is also observed, except that the low-pressure area moves into the inlet chamber of the rotor. In Fig. 7 the averaged relative velocity distribution around the blades (in the middle of channel width) is presented.

The comparison was made for the four operating states in the fan performance curve, i.e. the nominal flow, one over-nominal and two sub-nominal conditions.

For the nominal flow rate (0.72 kg/s), relative velocity profile for all the 9 impeller blades is almost identical, thus the distribution of shear stresses and losses are uniform. The same situation applies to the distribution of normal stresses resulting from the static pressure distribution at the nominal point (Fig. 6).

Adding resultant forces derived from normal and shear stresses acting on the blades in nominal flow conditions, the local static equilibrium with the central system of forces and their moments is obtained. The lack of symmetry in the pressure distribution and relative flow velocity for the off-design states causes non-uniform loads of the impeller shaft and leads to the generation of noise vibrations and deterioration of fan performance. It also has a negative impact on the acoustics of the machine.

The non-uniform distribution of velocities in radial cascade flow has a direct relationship with the vortices emerging in the blade channels. These structures are presented in Fig. 8, projecting the streamlines on a transverse plane in the middle of the impeller outlet width. The relative vortex in a channel doesn't appear close to the nominal operating conditions. For the nominal point, the streamlines are almost aligned to the blade centre line (zero incidences). During the sub-nominal operation, some opposite circulation vortices are created with respect to the impeller rotation. With the further throttling, the vortices cover the entire area of the blade passage on the suction-side of the impeller blades. In the case of over-nominal flow rate, the opposite circulation vortices were observed on the pressure-side of the rotor blades.

Conclusions

The complex, 3D, and unsteady flow through the centrifugal fan is difficult to be clearly resolved in a theoretical way. As a result, the common theme in the literature is a simplified way of describing energy transfer and flow phenomena occurring in this type of rotating machinery. The actual flow is reduced to the simple plane system, and then using basic equations and adequate loss and efficiency models the average parameters in the selected sections are determined. The analytical methods are not precise and often provide results that are significantly different from reality, and prediction of fan performance is almost impossible. At the same time, the opportunities for direct mea-

surement of the flow parameters in rotating blade channels are limited and require expensive research tools (e.g., LDA).

Our paper proposes a more modern tool for assessing the complete flow characteristics and performance of the machine based on the finite volume method (FV) ANSYS CFX [10] software. Calculations carried out on the basis of the developed numerical model fully support a good convergence of analytical solutions to the real characteristics of the machine. The simulation using CFD techniques allows us to obtain not only primary indicators of the fan (pressure rise, efficiency, power consumption), but also illustrates the characteristics of the flow structure in the machine. Poorly shaped flow generates numerous losses relating to the change of flow direction, separation regions, mixing and viscous losses, etc. The study documented a real physically correct impact of the internal flow structure on the fan operation conditions and performance. It is expected that CFD methods will become a necessary and important part of turbo machinery design and optimization, especially in the increasingly stringent technical-economic requirements and environmental conditions, including in those concerning energy efficiency and acoustic characteristics.

Acknowledgements

This paper was carried out under contract (11.11.210.216) AGH University of Science and Technology, Faculty of Fuels and Energy, Kraków, Poland.

References

1. DIXON S.L., HALL C.A. Fluid mechanics and thermodynamics of turbomachinery. 6th Edition. Elsevier **2010**.
2. GUO E.-M., KIM K.-Y. Three-dimensional flow analysis and improvement of slip factor model for forward-curved blades centrifugal fan. *Journal of Mechanical Science and Technology*. 04/**2012**.
3. FORTUNA S. The investigation of the useful work and losses in radial fans. Monographs, AGH University of Science and Technology Press, Krakow **2011** [In Polish].
4. COMMISSION REGULATION (EU) No. 327/2011 of 30 March **2011**.
<http://eur-lex.europa.eu/LexUriServ/LexUriServ.do?uri=OJ:L:2011:090:0008:0021:en:PDF>.
(ANSI/AMCA Standard 205-12. Energy Efficiency Classification for Fans. An American National Standard Approved by ANSI on May 4, **2012**).
5. CEBECI T., SHAO J.P., KAFYEKE F., LAURENDEAU E. *Computational fluid dynamics for engineers*. Springer V. **2005**.
6. GAŠPAROVIČ P., ČARNOGURSKÁ M. Aerodynamic optimisation of centrifugal fan casing using CFD. *Journal of Applied Science in the Thermodynamics and Fluid Mechanics* **2**, (1), 1802, **2008**.
7. ATRE PRANAV C., THUNDIL KARUPPA RAJ R. Numerical Design and Parametric Optimization of Centrifugal Fans with Airfoil Blade Impellers. *Research Journal of Recent Sciences*. **1**, (10), 7-11, October **2012**.
8. YOUNSI M., BAKIR F., KOUIRDI S., REY R. 3D unsteady flow in a centrifugal fan: impeller – volute interaction. *Journal of Computational and Applied mechanics*. **8**, (2), 211, **2007**.
9. ANSYS CFX-Solver Theory Guide. Release 14.0. November **2011**.
10. MENTER F. R. Two-Equation Eddy-Viscosity Turbulence Models for Engineering Applications, *AIAA Journal*, **32**, (8), 1598, **1994**.